

78

Plastic flow in close-packed crystals via nonequilibrium molecular dynamics

Anthony J. C. Ladd

Department of Applied Science, University of California at Davis, Davis, California 95616

William G. Hoover

*Department of Applied Science, University of California at Davis—Livermore, Livermore, California 94550
and Lawrence Livermore National Laboratory, Livermore, California 94550*

(Received 4 April 1983)

The measurement of plastic-wave profiles in strong shock waves suggests a power-law dependence of the solid-phase shear stress on strain rate. The strain rates in these experiments vary from about 10 kHz to 0.1 GHz. We have carried out molecular-dynamics simulations of steady-state plastic flow in two- and three-dimensional close-packed crystals, using recently developed "nonequilibrium" equations of motion to maintain a constant strain rate and temperature. These calculations appear to be consistent with current experimental data and suggest that the flow of close-packed metals is described by a single physical mechanism over a range of strain rates from 10 kHz to 1 THz.

I. INTRODUCTION

The use of laser interferometry to measure particle velocities¹ has enabled accurate shock-wave profiles to be determined for rise times of the order of 1 nsec.² Shock-wave experiments on samples of different thicknesses have established that steady plastic waves are formed, with rise times that can be measured optically for pressures up to 1 Mbar.² These high-pressure experiments have extended the experimentally accessible range of strain rates by 5 orders of magnitude, to about 0.1 GHz.

Grady's analysis of plastic-wave shapes in aluminum suggests that the shear stress increases as, approximately, the square root of the strain rate.³ His theoretical model, based on the idea of shear bands with heat flowing from the bands according to a diffusion equation, is consistent with a square-root dependence of the shear stress on strain rate.³ A different analysis of the same data, by Wallace, predicts a shear stress larger by about 2 orders of magnitude, and a weaker power-law dependence on strain rate.⁴ Such discrepancies indicate the uncertainties involved in estimating shear stress from shock-wave profiles.

It is well known that plastic flow in crystals proceeds through defect, primarily edge dislocation, motion.⁵ Semiempirical theories have been successful in correlating experimental data obtained in low-strain-rate tension tests,⁶ but it has been known for some time that these theories underestimate stress relaxation in plastic shock waves.⁷ The rate of dislocation multiplication is too small by several orders of magnitude.

At low strain rates, below 10 kHz, grain structure, impurities, and other material-dependent properties dominate plastic flow, but a universal flow behavior is expected at high strain rates, at least in close-packed crystal structures. It has been our goal to elucidate some of the fundamental aspects of high-strain-rate plastic flow by molecular-dynamics simulation. A preliminary account of this work, including details of the equations of motion has already been published.⁸

II. RESULTS

The isothermal equations of motion described in Ref. 8 have been applied to simulations of steady Couette flow in monatomic close-packed crystals. These crystals are comprised of point particles interacting via a pairwise additive, piecewise linear force law.⁹ The zero-force separation is d_0 , and the force constant is κ . The attractive force is greatest at $r = d_0 + w$, and decreases linearly to zero at $r = d_0 + 2w$. In our calculations, the width parameter $w = 0.15d_0$. The equation of state of the two-dimensional triangular lattice has been characterized by computer simulation.¹⁰ The temperature dependences of the internal energy, pressure, and Lamé constants¹⁰ are summarized in Table I. We have found the melting point of the triangular lattice from a plot of energy versus temperature, at constant volume. A flat tie line was observed, giving a melting point

$$kT_m / \kappa d_0^2 = 0.0135 \pm 0.0005$$

at a density

$$\rho = \frac{3}{4}^{1/2} N d_0^1 / V = 1.1.$$

Simulations at zero degrees have shown that the dislocation propagation velocity in this lattice is insensitive to

TABLE I. Thermodynamic and elastic properties of the triangular lattice. The Lamé constants were obtained by molecular-dynamics simulations of strained crystals. Results at intermediate temperatures can be estimated by interpolation ($\rho = 1.1$).

$kT/\kappa d$	$\Phi/N\kappa d_0^2$	p/κ	η/κ	λ/κ
0	-0.0643	0.085	0.37	0.54
0.004	-0.0602	0.080	0.37	0.53
0.008	-0.0560	0.077	0.36	0.51
0.012	-0.0514	0.075	0.31	0.51

stress once the rather large Peierls strain (~ 0.05) is overcome.¹¹ At higher temperatures we have found that the Peierls strain is reduced, but the propagation velocity is similar, approximately $0.3(\kappa/m)^{1/2}d_0$, or about one-half the transverse sound speed. Finally, the energy and stress of small groups of dislocations has been determined.⁹ Analogous results for the three-dimensional lattices are not yet available.

We have investigated the effects of dimensionality, system size, density, temperature, and strain rate on the internal energy and stress tensor. The two- and three-dimensional stress tensors have been compared with each other and with results deduced from laser interferometry measurements of shock-wave profiles in closed-packed metals.²⁻⁴ We have compared the results in two dimensions with theoretical predictions based on a model of a dilute "gas" of point dislocations.¹²

A. Two dimensions

At each density, temperature, and strain rate studied, results were obtained for systems of 64–400 atoms. The calculations were run up to strains of at least 10 in each case, which was sufficient to establish a steady state and reduce statistical errors in the shear stress and internal energy to a few percent. The fluctuations in the normal stresses were larger. A typical set of results is shown in Table II for a density $\rho=1.1$ and temperature $kT/\kappa d_0^2=0.008$. An estimate of the statistical uncertainties can be obtained from the two sets of results at $\dot{\epsilon}=0.05(\kappa/m)^{1/2}$, $N=144$. The potential energy of the crystals does not exhibit any statistically significant number dependence. At low strain rates, there is number dependence in the stress tensor, caused by large fluctuations in the dislocation density between states with no dislocations and states with a single dislocation pair. The smallest system size that requires a pair of dislocations to be permanently present can be estimated from the plastic strain rate $\dot{\epsilon}=bv\rho_D$, where ρ_D is the dislocation number

density. Using our estimate of the dislocation propagation velocity, $v=0.3(\kappa d_0^2/m)^{1/2}$, we find $N_{\min}\sim 0.7\dot{\epsilon}^{-1}(\kappa/m)^{1/2}$. This fits nicely with our simulation results, where at a strain rate of $0.01(\kappa/m)^{1/2}$, the 64-particle system is anomalous and where at a strain rate of $0.005(\kappa/m)^{1/2}$ both 64- and 144-particle results are different from $N=256$. These estimates indicate that results at strain rates of $0.001(\kappa/m)^{1/2}$ would require about 700 atoms.

A summary of our two-dimensional results is contained in Table III. The pressure shift Δp is the difference between the hydrostatic pressure at the given strain rate and that at the same density and temperature, but at zero strain rate. The thermal pressures used are given in Table I. The dislocation energy Φ_D is obtained from the potential energy per particle by subtracting the potential energy of the equilibrium crystal at the appropriate density and temperature (Table I), and the shear energy due to the mean shear stress σ_{xy} , given by $\Phi_S=(V/2)\sigma_{xy}^2/\eta$. This is consistent with the elastic theory of dislocations in periodic systems.^{9,13} We made a few calculations at a density equal to 1, but the results were not significantly different from those at $\rho=1.1$. This work concentrates on the temperature and strain-rate dependence.

The shear stress at each temperature is well represented by a power-law dependence on strain rate of the form

$$\sigma_{xy} \propto (\dot{\epsilon} \sqrt{m/\kappa})^{\gamma(T)}.$$

The exponent γ is almost linear in the temperature. If the temperature-dependent Lamé constants calculated earlier are used to determine the dislocation strength parameter D ,⁵

$$D(T) = (\eta/\pi)(\lambda + \eta)/(\lambda + 2\eta),$$

then γ is almost exactly given by

$$\gamma = 3kT/Db^2.$$

Molecular-dynamics data, together with the fitted curves are shown in Fig. 1. The theoretical significance of the

TABLE II. Number dependence of molecular-dynamics simulations of two-dimensional steady Couette flow at a density $\rho=1.1$. The potential energy and stress tensor quoted are relative to those at zero temperature and strain rate.

$\dot{\epsilon}(m/\kappa)^{1/2}$	N	$\Delta\Phi/N\kappa d_0^2$	$\Delta\sigma_{xx}/\kappa$	$\Delta\sigma_{yy}/\kappa$	σ_{xy}/κ
0.005	64	0.0121	0.021	0.008	0.028
	144	0.0123	0.017	0.011	0.027
	256	0.0127	0.017	0.012	0.024
0.01	64	0.0136	0.024	0.007	0.032
	144	0.0139	0.020	0.013	0.027
	256	0.0141	0.020	0.012	0.026
0.02	144	0.0156	0.022	0.011	0.032
0.05	64	0.0197	0.026	0.010	0.043
	144	0.0197	0.030	0.009	0.041
	144	0.0192	0.029	0.012	0.042
0.1	64	0.0238	0.042	0.004	0.056
	400	0.0243	0.043	0.005	0.054

TABLE III. Molecular-dynamics simulation of two-dimensional steady Couette flow at a density $\rho=1.1$. The thermal contributions to the pressure and potential energy have been removed, using the equation of state given in Table I. The energy due to the average shear stress $\Phi_S=(V/2)\sigma_{xy}^2/\eta$ is also subtracted from the potential energy to give Φ_D . The stress σ_1 is the normal stress difference $\sigma_{xx}-\sigma_{yy}$.

$kT/\kappa d_0^2$	$\dot{\epsilon}(m/\kappa)^{1/2}$	σ_{xy}/κ	σ_1/κ	$\Delta p/\kappa$	$\Phi_D/N\kappa d_0^2$
0.004	0.005	0.042	0.010	-0.013	0.003
	0.01	0.043	0.018	-0.015	0.005
	0.02	0.051	0.022	-0.020	0.006
	0.05	0.064	0.047	-0.024	0.009
	0.1	0.065	0.068	-0.029	0.014
0.006	0.005	0.036	0.014	-0.010	0.003
	0.01	0.034	0.011	-0.012	0.005
	0.05	0.052	0.027	-0.018	0.010
	0.1	0.062	0.047	-0.022	0.013
0.008	0.005	0.024	0.005	-0.007	0.004
	0.01	0.026	0.008	-0.008	0.005
	0.02	0.032	0.011	-0.009	0.006
	0.05	0.041	0.019	-0.012	0.009
	0.1	0.054	0.038	-0.016	0.013
0.010	0.005	0.015	0.005	-0.004	0.005
	0.01	0.019	0.003	-0.005	0.006
	0.05	0.037	0.012	-0.007	0.010
	0.1	0.048	0.022	-0.010	0.013
0.012	0.005	0.008	0.001	-0.002	0.006
	0.01	0.011	-0.001	-0.003	0.007
	0.02	0.017	0.000	-0.003	0.008
	0.05	0.031	0.012	-0.002	0.010
	0.1	0.044	0.018	-0.005	0.012

temperature dependence of the exponent and its relation to theoretical predictions¹² are discussed later.

The convergence of the stress-strain-rate data at a shear stress $\sigma_0=0.079\kappa$ and a strain rate $\dot{\epsilon}_0=0.3(\kappa/m)^{1/2}$ indicates a general constitutive equation for high-strain-rate plastic flow,

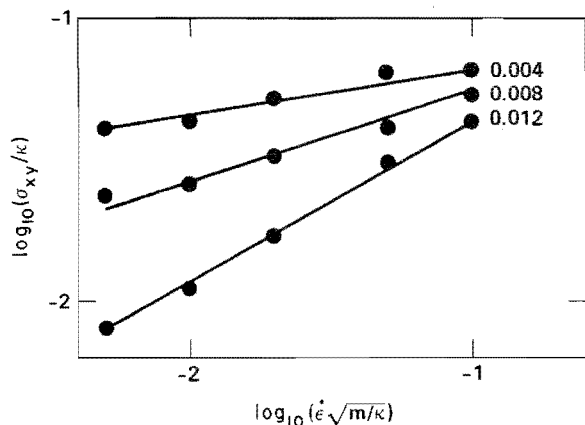


FIG. 1. Comparison of molecular-dynamics simulations of the shear stress as a function of strain rate with a power-law dependence of the form $\sigma_{xy}=A(T)\dot{\epsilon}^\gamma$, with $\gamma=3kT/Db^2$. The three lines correspond to temperatures $kT/\kappa d_0^2$ of 0.004, 0.008, and 0.012. They converge at a strain rate of $0.30(\kappa/m)^{1/2}$ and a stress of 0.079κ .

$$\sigma_{xy}(\dot{\epsilon}, T) = \sigma_0(\dot{\epsilon}/\dot{\epsilon}_0)^{\gamma(T)},$$

in good agreement with the molecular-dynamics data. A similar relation, with a linear dependence of γ on temperature, has been used by Sokolov¹⁴ to represent low-strain-rate data obtained from compression tests on several different metals. It is reasonable to assume that the point of convergence corresponds to a solid saturated with dislocations, and thus marks the transition to a different flow mechanism in which close-packed rows slide past each other with velocities dominated by the streaming contribution. Using this idea we can identify the phenomenological constants σ_0 and $\dot{\epsilon}_0$ with fundamental properties of the dislocations.

In a solid saturated with dislocations, the dislocation density is the same as the particle number density. The plastic strain rate $\dot{\epsilon}_0=bv(N/V)$ indicates a propagation velocity $v=0.25(\kappa d_0^2/m)^{1/2}$, which is consistent with other estimates.¹¹ The energy of a triangular lattice saturated with dislocations of alternate signs can be evaluated numerically⁹ with the result $\Phi=2\Phi_c-1.38Db^2$. The core energy Φ_c is $0.087\kappa d_0^2$.⁹ The elastic energy released by a pair is σb^2 , and thus the saturated solid is energetically favored for stresses greater than 0.076κ , when $\Phi-\sigma b^2 < 0$.

The statistical uncertainties in the normal stresses are larger than in the shear stress, and it is difficult to detect consistent trends in σ_{xx} and σ_{yy} . However, the normal stress difference $\sigma_{xx}-\sigma_{yy}$ exhibits a power-law depen-

dence on strain rate with a temperature-independent exponent of about 0.7. The pressure shift Δp has a similar dependence with a power of roughly 0.3. Our studies of dislocations in cold crystals⁹ revealed normal stress effects of similar magnitude to these, but they would be expected to be linear in the dislocation density, and therefore linear in the strain rate. The reason for these noninteger power-law dependencies is unclear.

The directions of maximum shear stress are almost parallel to the x and y axes, the largest deviation, occurring at low temperatures and high strain rates, being about 15° . This is consistent with a picture of plastic flow via the motion of edge dislocations in the x direction, which relieves the shear and rotational components of the strain rate simultaneously. Continuum theories generally assume that the plastic strain-rate directions are exactly parallel to the principal stress directions.

The dislocation energy is almost independent of temperature in the range $0.004 < kT/\kappa d_0^2 < 0.008$. At higher temperatures and low strain rates the energy increases slightly. This increase is probably due to excitation of low-frequency anharmonic oscillations of the dislocations, rather than to changes in the static elastic stress fields around them. The absence of a large temperature dependence in the dislocation energy indicates that the dislocation density and structure are insensitive to temperature. The variation in normal stresses is probably due to a reduction in the core stress with temperature.⁹ A temperature-independent dislocation density is in agreement with our observation of a temperature-independent dislocation propagation velocity.

B. Three dimensions

We have investigated plastic flow in a three-dimensional solid at two different strain rates: $\dot{\epsilon}(m/\kappa)^{1/2} = 0.01$ and 0.1 . The solid was initially a hexagonal close-packed lattice, with the sixfold axis perpendicular to the flow direction. We collected thermodynamic data but did not attempt to analyze the crystal structure of the steady-state

material. The analysis could perhaps be accomplished using Voronoi polyhedra but such a task would probably take longer than the simulations themselves. Most of the calculations were for 216 atoms; we could not detect statistically significant differences between $N=216$ and 512. The results reported here are all for $N=216$.

In these calculations the temperature slowly decreased due to truncation errors in solving the isothermal equations of motion. The cooling rate was slow,

$$\dot{T}/T \sim -10^{-4}(m/\kappa)^{1/2},$$

but substantial over typical runs of $2000(m/\kappa)^{1/2}$ to $10000(m/\kappa)^{1/2}$. In two dimensions, these truncation errors caused the system to heat up, but at a much slower rate, which, together with the shorter runs, did not significantly affect the results. The temperature drift could be overcome by occasional momentum rescaling. In analyzing these results we have divided them into batches, typically of times of $1000(m/\kappa)^{1/2}$, which are long enough to obtain meaningful statistical averages but short enough to be characterized by a single thermodynamic state. The results are collected in Table IV.

It can be seen from Table IV that the flow is qualitatively different at the two different strain rates. At the lower strain rate the flow is two dimensional; the solid is primarily sheared in the xy plane, parallel to the x axis. Both the shear stresses σ_{xy} and $\sigma_{xx} - \sigma_{yy}$ are comparable to the two-dimensional results. The dislocation energy, calculated without the small anharmonic corrections to the energy of the unsheared crystal, is also similar to the two-dimensional energies. At the higher strain rate the flow is characterized by temperature-independent shear stresses, a large normal stress in the zz direction, and a smaller dislocation contribution to the internal energy. The large shear stresses at the two highest temperatures are probably due to the shear-induced melting,¹⁵ resulting in a liquid state. It is not obvious what the high-strain-rate flow mechanism is, and a structural analysis of these plastically flowing solids would be of interest. At the

TABLE IV. Molecular-dynamics simulation of three-dimensional steady Couette flow at a density $\rho = Nd_0^3/V\sqrt{2} = 1.1$. The thermal contribution to the potential energy has been estimated from equipartition. The stresses σ_1 and σ_2 are the normal stress differences $\sigma_{xx} - \sigma_{yy}$ and $\sigma_{yy} - \sigma_{zz}$, respectively.

$\dot{\epsilon}(m/\kappa)^{1/2}$	$kT/\kappa d_0^2$	σ_{xy}/κ	σ_1/κ	σ_2/κ	p/κ	$\Phi_D/N\kappa d_0^2$
0.01	0.0010	0.050	0.016	-0.003	-0.001	0.008
	0.0035	0.038	0.008	0.000	0.002	0.007
	0.0066	0.029	0.006	0.001	0.004	0.008
	0.0079	0.022	0.007	0.000	0.005	0.006
	0.011	0.014	0.002	0.002	0.009	0.010
	0.012	0.012	0.004	0.001	0.009	0.011
0.1	0.0029	0.035	0.026	0.048	0.021	0.002
	0.0038	0.035	0.025	0.038	0.020	0.001
	0.0048	0.032	0.025	0.032	0.019	0.000
	0.0058	0.032	0.026	0.032	0.018	0.001
	0.0068	0.032	0.028	0.027	0.016	0.003
	0.011	0.056				
	0.012	0.053				

lower strain rate it is presumably slippage of the basal planes over each other.

C. Scaling laws and comparison with experiment

The most important characterization of a plastically flowing solid is the constitutive law for the shear stress as a function of density and temperature. In this section we describe a scaling relation that can be used to compare our simulation results with estimates deduced from shock-wave experiments.²⁻⁴ The natural dimensionless variables are T/T_m , $\dot{\epsilon}d/c_T$, and σ_{xy}/η , where T_m is the melting temperature, d is a characteristic interatomic distance, c_T is the transverse sound speed, and η is the shear modulus. For simplicity we have used the zero-temperature moduli in scaling the simulation data. The three-dimensional simulations involve the shearing of basal planes. The appropriate shear modulus, $\eta = C_{55} - p = 0.408$, is used to scale the shear stresses. The experimental materials are polycrystalline characterized by an average isotropic shear modulus. The results of the scaling are illustrated in Fig. 2.

The two-dimensional results are shown by solid lines, corresponding to temperatures of $0.3T_m$, $0.6T_m$, and $0.9T_m$, and are extrapolated with dashed lines to lower strain rates where estimates are available from interpretation of shock-wave profiles. The experimental results include Wallace's calculations for aluminum.⁴ These calculations are based on a continuum model, fitted to plastic-wave data and consistent with reasonable thermodynamic bounds on the temperature, stress, and entropy within

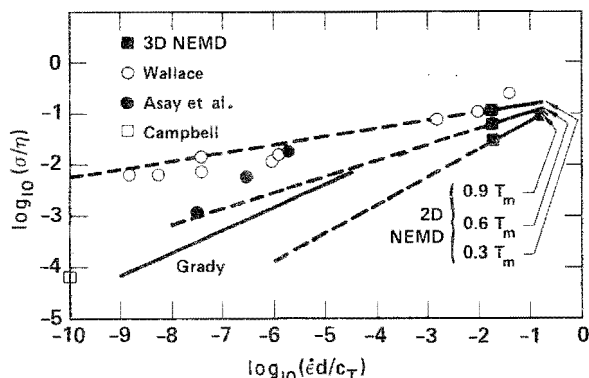


FIG. 2. Strain-rate dependence of the shear stress. η is the shear modulus, d the nearest-neighbor spacing in a close-packed lattice, $\dot{\epsilon}$ the strain rate du_x/dy , and c_T the transverse sound velocity. The nonequilibrium molecular dynamics was generated for two-dimensional solids at 1:1 times the stress-free density and temperatures of 0.3 (top solid line), 0.6 (middle line), and 0.9 (bottom line) times the melting temperature, using from 64 to 400 particles. The scaled three-dimensional simulation results, at corresponding density and temperatures, are shown as solid squares. The melting temperature of the three-dimensional crystal was assumed to be $0.012\kappa d_0^3/\kappa$, and the required reduced temperatures were obtained by interpolating the data in Table IV. The beryllium data from Asay *et al.*, Wallace and Grady's estimates for aluminum, and Campbell's older low-strain-rate estimate are shown. The uncertainty in the slope of the lines is a few percent.

nonequilibrium shock waves. The low-strain-rate data ($10^{-10} < \dot{\epsilon}d/c_T < 10^{-6}$) are taken from weak shock-wave experiments (21–89 kbar), where the change in thermodynamic state is small. The temperature, 300–400 K, corresponds to about one-third the melting temperature of aluminum. The agreement between these results and our $0.3T_m$ line is good. The high-strain-rate results are from strong shocks (~ 1 Mbar) where the thermodynamic state is not well specified. The discrepancies between Wallace's and Grady's less sophisticated estimates, from the same experimental profiles, reflect the difficulty in estimating shear stress from measured longitudinal profiles. Asay's calculations for beryllium² likewise include some uncertain approximations. The upper bounds for shear stress, computed for aluminum, copper, and iron by Chhabildas and Asay,² lie well above our low-temperature line.

The approximate methods used to estimate shear stress in Refs. 3 and 4 are oversimplifications of complex phenomena, but they represent the best available experimental description of the dependence of shear stress on strain rate. The agreement between these results and the simulation data suggests that a common explanation of high-strain-rate plastic flow (strain rates exceeding 10 kHz) can be obtained from an analysis of the two-dimensional simulation results.

III. THEORY

We consider a simple model of plastic flow, involving a two-dimensional "gas," of point dislocations, propagating in an elastic continuum at constant strain rate and temperature. In this model, free dislocations can be nucleated from bound pairs, by an external stress field. We use a simplified but fundamentally similar approach to that used by Bruinsma *et al.*,¹² to calculate the nucleation rate at constant stress. In addition, we consider the effect of stress fluctuations, which can increase the rate of recombination of free dislocations into bound pairs. Inclusion of these stress fluctuations is essential to bring the predictions of this model into agreement with the simulation results.

A pair of dislocations on the same glide plane with Burgers vectors $(\pm b, 0)$, subject to an external shear stress $\sigma_{xy} = \sigma$, move in a potential

$$\Phi(r) = 2\Phi_c + Db^2[\ln(r/b) - 1] - \sigma br,$$

where Φ_c is the core energy. This equation, which can be derived from continuum elastic theory, has been validated by atomic simulations.⁹ The potential has a maximum when $r = Db/\sigma$, and therefore, the rate of nucleation of free dislocations from bound pairs can be calculated from an Arrhenius rate law,

$$R_+ \propto \exp(-\Phi_{\max}/kT) \propto \sigma^{Db^2/kT}.$$

A more sophisticated calculation, including the change in potential when the dislocations are not on the same glide plane, leads to the same dependence of the nucleation rate on shear stress.¹²

At steady state, the nucleation rate is equal to the recombination rate

$$R_- \simeq x_c \nu \rho_D^2 \simeq x_c \nu (\dot{\epsilon}/bv)^2,$$

where x_c is the capture cross section proportional to

$\sigma^{-1.12}$ Since $Db^2 \gg kT$, this model predicts a stress-strain-rate relation of the form

$$\sigma \propto \dot{\epsilon}^{2kT/Db^2},$$

whereas the observed power is $3kT/Db^2$. This discrepancy may be due to stress fluctuations caused by the time delay in transmitting plastic strain from a moving dislocation.

Plastic strain is initially generated as a discontinuity in the displacement field, localized behind the moving dislocation. It spreads out as shear waves at a rate determined by the transverse sound speed. The plastic strain is transmitted over a distance comparable to the mean separation between dislocations, approximately $\rho_D^{-1/2}$, with a corresponding transmission time of $c_T^{-1}\rho_D^{-1/2}$. Thus the characteristic frequency ω and amplitude $\Delta\sigma$ of the stress fluctuations are

$$\omega \sim c_T(\dot{\epsilon}/bv)^{1/2} \propto (\dot{\epsilon})^{1/2}$$

and

$$\Delta\sigma \sim \eta\dot{\epsilon}/\omega \propto (\dot{\epsilon})^{1/2}.$$

The stress fluctuations in this picture are sawtoothed rather than sinusoidal. The shear stress rises linearly in time, until it is sharply reduced by a passing dislocation.

At low strain rates the average spacing between dislocations $\rho_D^{-1/2}$ is much larger than the capture cross section x_c . Recombination takes place via dislocation motion, resulting in the expression given earlier for the recombination rate. At high strain rates when the dislocation density is relatively large, the average spacing is comparable to the capture radius. It is possible that under these conditions, recombination occurs, predominantly after a passing dislocation has reduced the local stress, thus increasing the effective capture area. Thus recombination becomes a "three-body" process at high strain rates with a rate pro-

portional to ρ_D^3 , leading to the stress-strain-rate relation

$$\sigma \propto \dot{\epsilon}^{3kT/Db^2}$$

observed in the simulations.

IV. DISCUSSION

In this work we have presented numerical results for high-strain-rate steady Couette flow in simple crystalline solids. The results have only a small number dependence for unit cells greater than 50 atoms, and we have found an unambiguous power-law dependence for the shear stress on strain rate in two-dimensional crystals. The power is of the noninteger type, varying approximately linearly with temperature up to a maximum of just over 0.5 at melting. The power is 1 in "Newtonian" liquids, and 0 in perfect plasticity. It is intriguing and probably significant that the power varies almost exactly as $3kT/Db^2$. Development of our qualitative explanation of this observation presents an interesting theoretical challenge.

We have found a simple scaling relation linking our computer-simulation results to estimates based on experimental shock-wave data. Both simulation and experimental data closely obey this corresponding states principle. This strongly suggests a universal mechanism for high-strain-rate flow in close-packed structures, independent of dimensionality force law or impurities. It would be of interest to develop plastic constitutive laws based on these simulation results.

ACKNOWLEDGMENTS

This work was supported in the Department of Applied Science by the United States Army Research Office, Research Triangle Park, North Carolina, and by the United States Department of Energy at Lawrence Livermore National Laboratory under Contract No. W-7403-Eng-48.

¹L. M. Barker, in *Behavior of Dense Media Under High Dynamic Pressures* (Gordon and Breach, New York, 1968), p. 483. For a review of earlier work, see J. C. Campbell, *Mater. Sci. Eng.* **12**, 3 (1973).

²L. C. Chhabildas and J. R. Asay, *J. Appl. Phys.* **50**, 2749 (1979). J. R. Asay, L. C. Chhabildas, and J. L. Wise, in *Shock Waves in Condensed Matter—1981 (Menlo Park)*, Proceedings of the Conference on Shock Waves in Condensed Matter, edited by W. J. Nellis, L. Seaman, and R. A. Graham (AIP, New York, 1982), pp. 417 and 427.

³D. E. Grady, *Appl. Phys. Lett.* **38**, 825 (1981); D. B. Hayes and D. E. Grady, in *Shock Waves in Condensed Matter—1981 (Menlo Park)*, Proceedings of the Conference on Shock Waves in Condensed Matter, edited by W. J. Nellis, L. Seaman, and R. A. Graham (AIP, New York, 1982), p. 412.

⁴D. C. Wallace, *Phys. Rev. B* **22**, 1477 (1980); **22**, 1487 (1980); **24**, 5597 (1981); **24**, 5607 (1981). See also P. W. Bridgman, *Rev. Mod. Phys.* **22**, 56 (1950).

⁵A. H. Cottrell, *Dislocations and Plastic Flow in Crystals* (Clarendon, Oxford, 1953); F. R. N. Nabarro, *Theory of Crystal Dislocations* (Clarendon, Oxford, 1967); *Dislocation*

Dynamics, edited by A. R. Rosenfield, G. T. Hahn, A. L. Bement, and R. I. Jafee (McGraw-Hill, New York, 1968); X. Markenscoff and R. J. Clifton, *J. Mech. Phys. Solids* **22**, 253 (1981); for recent work, see *Dislocation Modelling of Physical Systems*, edited by M. F. Ashby, R. Bullough, and C. S. Hartley (Pergamon, New York, 1980).

⁶W. G. Johnston and J. J. Gilman, *J. Appl. Phys.* **31**, 632 (1960); J. J. Gilman, *Micromechanics of Flow in Solids* (McGraw-Hill, New York, 1969).

⁷J. R. Asay, G. R. Fowles, G. E. Duvall, M. H. Miles, and R. F. Tinder, *J. Appl. Phys.* **43**, 2132 (1972).

⁸W. G. Hoover, A. J. C. Ladd, and B. Moran, *Phys. Rev. Lett.* **48**, 1818 (1982). Replace the misprint $\partial \dot{l} / \partial l$ on p. 1819 with $\partial \dot{p} / \partial p$.

⁹A. J. C. Ladd and W. G. Hoover, *Phys. Rev. B* **26**, 5469 (1982). The right-hand sides of Eqs. (3) should be multiplied by the force constant κ .

¹⁰W. G. Hoover, A. J. C. Ladd, and N. E. Hoover, in *Interatomic Potentials and Crystalline Defects*, edited by J. K. Lee (Metallurgical Society, Warrendale, Pennsylvania, 1981); A. J. C. Ladd and W. G. Hoover, *J. Chem. Phys.* **74**, 1337 (1981).

¹¹W. G. Hoover, N. E. Hoover, and W. C. Moss, *J. Appl. Phys.* 50, 829 (1979).

¹²R. Bruinsma, B. I. Halperin, and A. Zippelius, *Phys. Rev. B* 25, 579 (1982).

¹³D. S. Fisher, B. I. Halperin, and R. Morf, *Phys. Rev. B* 20,

4692 (1979).

¹⁴L. D. Sokolov, *Dokl. Akad. Nauk SSSR* 67, 459 (1949) [*Sov. Phys.—Dokl.* 67, 459 (1949)]; S. K. Samanta, *Int. J. Mech. Sci.* 11, 433 (1969).

¹⁵D. J. Evans, *Phys. Rev. A* 25, 2788 (1982).